ACS OMEGA

http://pubs.acs.org/journal/acsodf

Article

Trilobatin, an Active Dihydrochalcone from *Lithocarpus polystachyus*, Prevents Cisplatin-Induced Nephrotoxicity via Mitogen-Activated Protein Kinase Pathway-Mediated Apoptosis in Mice

Yue-yang Duan, Xiao-jie Mi, Wen-ya Su, Shan Tang, Shuang Jiang, Zi Wang, Li-Chun Zhao,* and Wei Li*

Cite This: *ACS Omega* 2022, 7, 37401−37409

Read Online

ACCESS | Metrics & More | Article Recommendations

ABSTRACT: Although naturally occurring flavonoids have shown beneficial effects on the side effects caused by cisplatin, there are few reports on the protective effect of dihydrochalcone on the cisplatin-induced toxicity. Trilobatin (TLB), as the major sweetener and active ingredient in *Lithocarpus polystachyus* Rehd, is a dihydrochalcone-like compound that can be present in concentrations of up to 10% or more in tender leaves. Herein, a cisplatin-induced acute kidney injury (AKI) model was established to investigate the protective effect and mechanism of TLB against the cisplatin-induced nephrotoxicity in mice. The results showed that TLB significantly reversed the inhibition of CRE, BUN, and MDA levels compared with the cisplatin group. Furthermore, TLB treatment (50 and 100 mg/kg) for 10 days significantly alleviated cisplatin-induced renal pathological changes. TUNEL staining showed that TLB administration can effectively improve the occurrence of apoptosis of renal tissue cells caused by cisplatin exposure. Importantly, western blot analysis verified that TLB alleviated cisplatin-induced nephrotoxicity by regulating the AKT/MAPK signaling pathway and apoptosis. In summary, our findings showed clearly that TLB has a significant preventive effect on cisplatin-induced AKI.

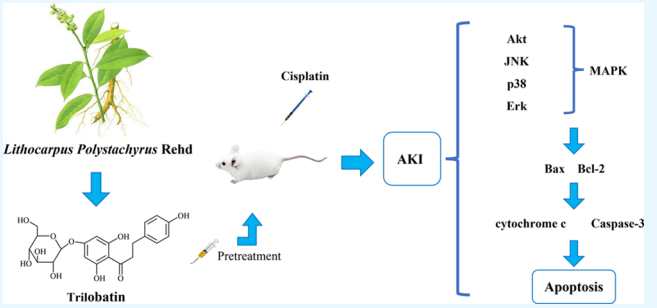

1. INTRODUCTION

Lithocarpus polystachyus Rehd (LPR, Figure 1A), also known as sweet tea, is an evergreen tree of the genus Quercus in the family Fagaceae. LPR is a common tea beverage and folk health care product in southwest China with rich flavonoids and tea polyphenols and has a high application value in the fields of new drugs and functional foods.[1−5] Trilobatin (TLB, Figure 1B), a strong natural sweetener, is a novel glycosylated dihydrochalcone isolated from the leaves of LPR and has been reported to have antioxidant properties.[6]

Acute kidney injury (AKI), often resulting from ischemic, nephrotoxic, and septic insults, is a devastating clinical condition that can result in short-term and long-term complications, including chronic kidney disease, end-stage renal disease, and death.[7,8] Cisplatin has been known as one of the most applicable anticancer agents that is usually used in the treatment of malignancies.[9−12] It was widely applied to the treatment of many solid tumors in ovary, breast, lung, cervix, and many other tissues.[13] Severe and recurrent cisplatin-induced AKI as part of standard cancer therapy is a known risk factor for cancer patients. Approximately one third of patients who receive cisplatin therapy develop AKI, which has limited the clinical application of cisplatin on solid tumors.[14] AKI is characterized by tubular damage and renal function decline.[15] During this process, cisplatin accumulates in the kidney tubular epithelial cells and injures the cells through various pathways, among which oxidative stress is a major factor.[16] Furthermore, mitochondrial fragmentation is a crucial mechanism contributing to tubular cell apoptosis during AKI.[17] Hence, targeting protection against oxidative stress and mitochondria-related apoptosis could be essential for the adjunctive therapies to reduce morbidity and mortality in cancer patients.

TLB is a flavonoid compound with high content in LPR. It is reported that flavonoid compounds have anti-inflammatory activity through their ability to scavenge reactive oxygen species (ROS).[18] The ROS produced after cisplatin stimulation can activate a series of downstream proteins that

Received: July 1, 2022
Accepted: August 31, 2022
Published: October 13, 2022

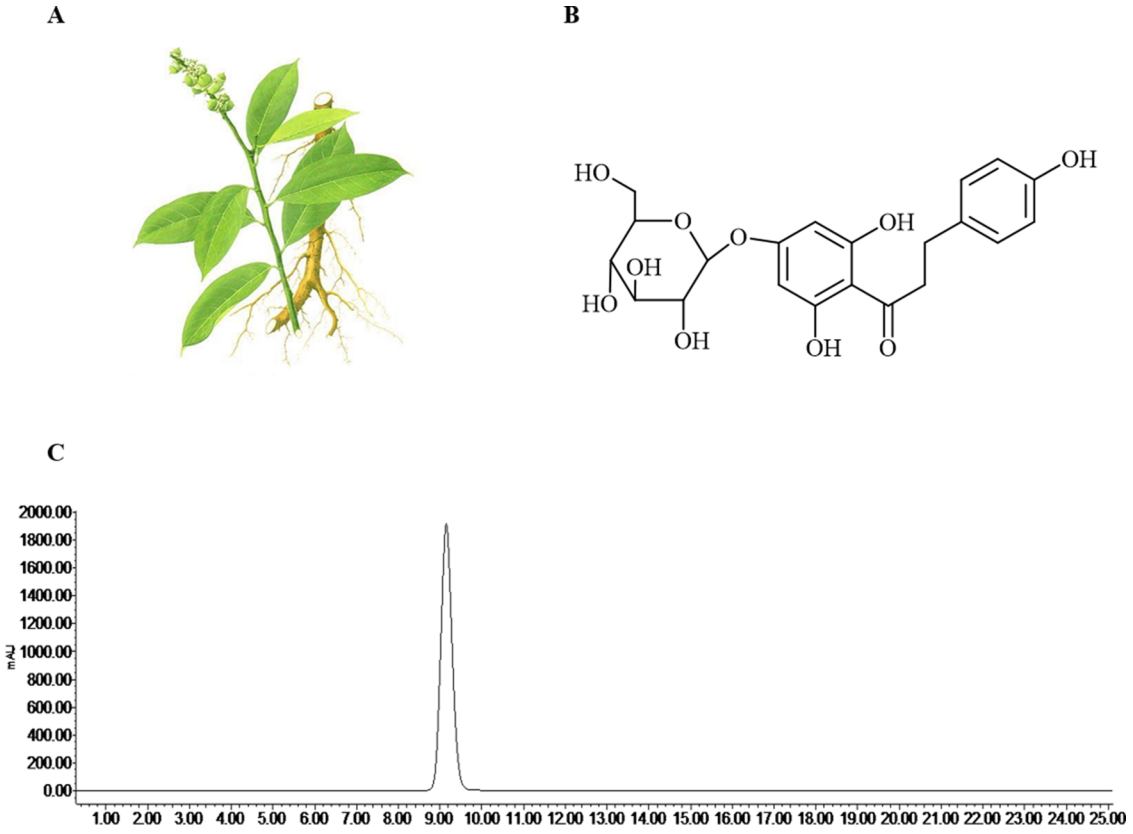

Figure 1. Picture of *Lithocarpus polystachyus* Rehd (A), chemical structure of TLB (B), and high-performance liquid chromatography (HPLC) chart of TLB (C).

mediate necrosis and apoptosis, especially the mitogen-activated protein kinase (MAPK) family proteins. The MAPK family consists of three main serine/threonine kinase proteins, including JNK, Erk, and p38, which are related to cell proliferation and differentiation and are widely associated with inflammation, apoptosis, and cell death.[19] Past studies have shown that the members of the MAPK family, like c-Jun N-terminal kinase (JNK), extracellular signal regulated kinase (Erk), and p38, are activated following cisplatin exposure, which further results in renal cell death.

Therefore, in this study, we established a cisplatin-induced AKI model in mice and evaluated the protective effect of TLB pretreatment on renal toxicity in mice by inhibiting oxidative damage and apoptosis.

2. MATERIALS AND METHODS

2.1. Chemical Compounds and Reagents. The tender leaves of LPR were obtained from Hunan Zhijiang Funong Sweet Tea Co., Ltd. and were identified as LPR by Professor Wei Li. The voucher specimen (No. 20160382) was reserved in the College of Chinese Medicinal Materials in Jilin Agricultural University. TLB (purity ≥ 98%) was made in the laboratory. The dried LPR leaves were crushed and screened, and ultrasonic-assisted extraction was performed with ethanol. TLB was preliminarily enriched in the extract by the macroporous resin purification technique. Then, the eluted component of 50% ethanol was extracted, and TLB was separated by semipreparative HPLC with purity ≥98% (Figure 1C).

Cisplatin (purity ≥ 99%) was purchased from Shanghai Siyu Chemical Technology Co., Ltd. (Shanghai, China). Hematoxylin−Eosin dye (H&E) was purchased from Shanghai Beyotime Biotechnology Co., LTD (Shanghai, China). Biological detection kits for BUN, CRE, MDA, GSH, SOD, and CAT were purchased from Nanjing Jiancheng Biological Research Institute (Nanjing, China). A TUNEL kit was purchased from Roche Biotechnology (Shanghai, China); the antibodies of rabbit monoclonal antimouse Bax, Bcl-2, cytochrome c, caspase-3, cleaved-caspase 3, and β-actin were recruited from Cell Signaling Technology (Danvers, MA, USA) or BOSTER Biological Technology (Wuhan, China). The antibodies against Akt, phospho-Akt (p-Akt), phospho-JNK(p-JNK), p38, phospho-p38 (p-p38), Erk, and phospho-Erk (p-Erk) were purchased from Wanlei Bio (Shenyang, China). All other reagents and chemicals, unless indicated, were obtained from Beijing Chemical Factory (Beijing, China).

2.2. Animals. Male ICR mice weighing 22−25 g (8-week-old) were purchased from YISI Experimental Animal Co., Ltd. with a Certificate of Quality No. SCXK (JI) 2018-0004 (Changchun, China). The animals were supplied with a standard laboratory diet and water ad libitum and maintained at 25 ± 2 °C and 60 ± 10% humidity with a 12 h light/dark cycle and acclimatized for 1 week prior to use. All experimental animal processing procedures were strictly performed in accordance with the Guide for the Care and Use of Laboratory Animals (Ministry of Science and Technology of China, 2006). All the animal experiments were approved by the Ethical Committee of Laboratory Animals of Jilin Agricultural University (2016-01-Permit Number: ECLA-JLAU 2016-016).

2.3. Experimental Design. The animals were randomly divided into four groups (n = 8): control group, cisplatin group (25 mg/kg), cisplatin + TLB 50 group (50 mg/kg), and

https://doi.org/10.1021/acsomega.2c04142
ACS Omega 2022, 7, 37401−37409

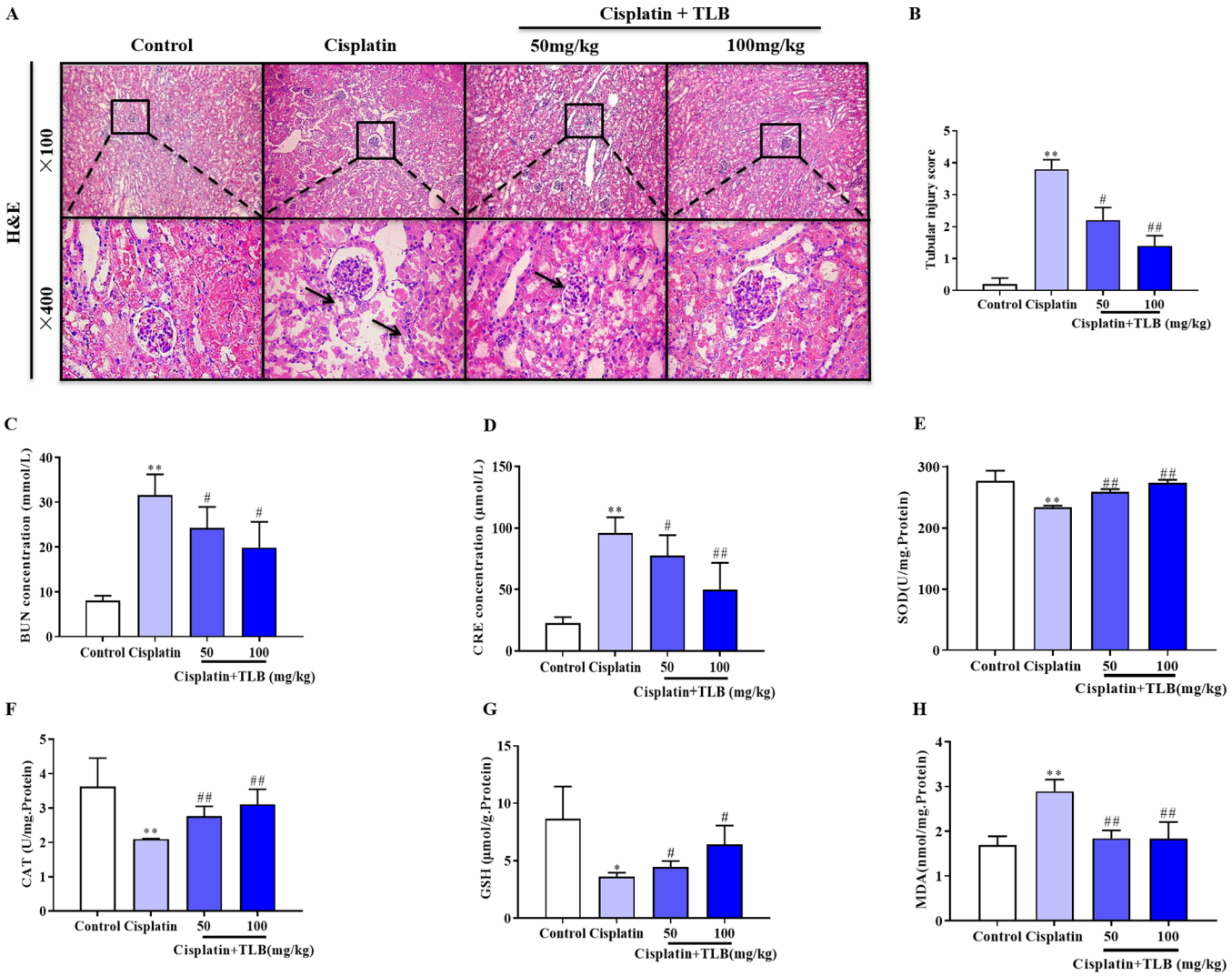

Figure 2. Pretreatment with TLB protected against cisplatin-induced renal histopathological injury in mice. Histological analysis of morphological changes in kidney tissues, which were stained with H&E (100×, 400×); arrows showed necrotic cell and inflammatory infiltrate cells (A). Column chart showed the renal tubular damage score (B). Effects of TLB on the levels of BUN (C) and CRE (D) in serum, and effects of TLB on contents of SOD (E), CAT (F), GSH (G), and MDA (H) in kidney tissues. All data were expressed as mean ± SD, $n = 8$. $^{*}p < 0.05$, $^{**}p < 0.01$ vs control group; $^{\#}p < 0.05$, and $^{\#\#}p < 0.01$ vs cisplatin group.

cisplatin + TLB 100 group (100 mg/kg). TLB and cisplatin were dissolved in 0.9% sterile saline. The dosage determination of TLB and cisplatin was based on our preliminary experiments and other previous studies.[1,20,21]

The mice of cisplatin + TLB 50 and cisplatin + TLB 100 groups were administered intragastrically with TLB (50 and 100 mg/kg per day) for 10 consecutive days, respectively. The mice of the control group were administered intragastrically with sterile saline during this period. On the seventh day, a single dose of cisplatin (25 mg/kg, diluted 0.9% saline) was i.p. injected to all the groups without the control group. At the end of the experiment, the mice were fasted overnight, and blood samples were collected through the retrobulbar vessels. Then, all animals were sacrificed, and organ samples were immediately dissected out, washed with cold saline, and measured for weight. The left kidney tissue was placed in a refrigerator at −80 °C for tissue homogenization and protein analysis. The right kidney tissues were fixed in 10% formaldehyde for tissue sections.

2.4. Determination of Biochemical Indicators. The serum BUN and CRE levels were measured according to the manufacturer's protocol. The left kidney was homogenized in 0.9% NaCl and centrifuged at 1000×*g* and 4 °C for 10 min. The supernatant was separated, and the GSH, MDA content, and SOD and CAT activities in renal tissue were determined according to the manufacturer's protocol (Nanjing Jiancheng Biotechnology Research Institute, Nanjing). The value of each sample is calculated according to the standard.

2.5. Histopathology Analysis. H&E staining was performed with 5 μm-thick sections of renal tissues. Histopathology changes were observed using a light microscope (Leica DM2500, Shanghai). The necrotic degree was assessed by the necrotic area, inflammatory cell infiltration degree, and congestion. Tubular injury scores were semi-quantitatively analyzed by counting the percent of tubules that displayed cell necrosis, tubule dilatation, loss of brush border, and cast formation, as follows: 0, none; 1, <10%; 2, 10% to 25%; 3, 25% to 75%; 4, >75%.

https://doi.org/10.1021/acsomega.2c04142
ACS Omega 2022, 7, 37401−37409

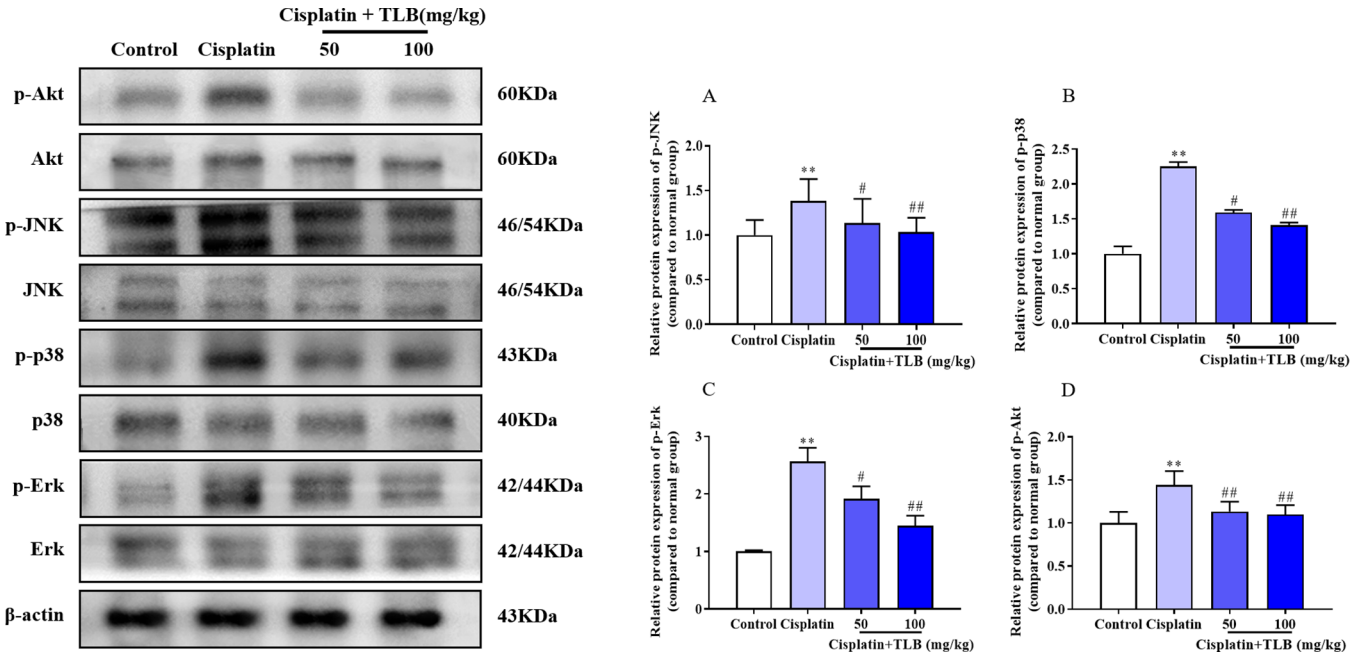

Figure 3. Pretreatment with TLB protected against renal oxidative stress induced by cisplatin. Effect of TLB on the expression of the MAPK signaling pathway; the column chart shows antibody relative expression (A,B,C,D). The protein expression was examined by western blot analysis in kidney tissues from control, cisplatin, cisplatin + TLB (50 mg/kg), and cisplatin + TLB (100 mg/kg). All data were expressed as mean ± SD, n = 8. $^{**}p < 0.01$ vs control group; $^{\#}p < 0.05$, and $^{\#\#}p < 0.01$ vs cisplatin group.

2.6. TUNEL Staining. To measure the extent of apoptosis in the kidneys after cisplatin exposure, TUNEL evaluation was carried out as mentioned earlier with minor modification.[22] An in situ apoptosis detection kit (Mannheim, Germany) was used to assess apoptotic cells in the kidney tissues according to the manufacturer's instructions. First, a 5 μm-thick kidney paraffin section was deparaffinized and hydrated. Proteinase K (20 μg/mL) was added at room temperature and incubated for 10 min to permeabilize it, 0.3% H_2O_2 was added and incubated for 5 min to inactivate endogenous oxidase and incubated with the TUNEL mixture at 37 °C under dark conditions. Then POD and DAB staining solution were added successively and then stained with hematoxylin, and finally neutral gum was added to mount the slide. The expression of TUNEL-positive cells was observed under an optical microscope (Leica DM2500, Germany), and quantitative analysis was performed.

2.7. Immunofluorescence Analysis. Immunohistochemistry (IHC) of the paraffin sections was carried out according to the manufacturer's instructions (BOSTER Biological Technology, Wuhan, China). Xylene and aqueous alcohol solutions were used to deparaffinize and rehydrate paraffin slides. After antigen retrieval in a citrate buffer solution for 8 min, the sections were washed with PBS and incubated with 1% bovine serum albumin (BSA) for 20 min. The blocked serum was patted gently, and sections were incubated with primary antibodies containing Bax and Bcl-2 (1:100) at 4 °C overnight, respectively. After washing three times with PBS at room temperature, the secondary antibody solution was added to the sections and incubated at 37 °C for 30 min. Finally, 6 diamidino-2-phenylindole (DAPI) was used for nuclear staining. The fluorescence expressions were investigated using a fluorescence scanning microscope (Leica DM2500, Germany).

2.8. Western Blot Analysis. The kidney tissue protein samples extracted under the ultralow temperature state are fully dissolved in the preprepared RIPA lysis buffer, and the total protein concentration is detected using the BCA protein detection kit. The samples are separated by 12% SDS-PAGE gel, and the conjugated protein from the gel was transferred to the PVDF membrane. TBS and 0.1% Tween-20 mixture (TBST) were used to prepare 5% BSA blocking protein for 2 h, and then it washed with TBST three times, each time 10 min, and different bands were separated with the corresponding one. The antibody was incubated overnight at 4 °C: Akt (1:2000), p-Akt (1:2000), JNK (1:2000), p-JNK (1:2000), p-p38 (1:2000), p-38 (1:2000), p-Erk (1:2000), Erk (1:2000), Bax (1:2000), Bcl-2 (1:2000), cytochrome c (1:2000), caspase 3 (1:2000), cleaved-caspase 3 (1:2000), and β-actin (1:2000). Subsequently, membranes were rinsed three times with TBST for 10 min each time with gentle agitation and incubated with secondary antibodies. Finally, the membranes were visualized with the emitter coupled logic (ECL) plus western blot detection system (Media Cybernetics, State of California, USA).

2.9. Statistical Analysis. The results were expressed as the mean ± standard deviation (mean ± SD) of three independent experiments, and the differences were evaluated by one-way analysis of variance and the Tukey−Kramer multiple comparison test. Data were analyzed with Prism software V 9.0.0 (GraphPad, La Jolla, CA). Differences were considered to be statistically significant at values of $p < 0.05$ or $p < 0.01$.

3. RESULTS

3.1. TLB Ameliorated Cisplatin-Induced Renal Pathological Changes in Mice. As shown in Figure 2A, the renal cortex of the control group was normal and arranged regularly, the glomerulus and its surrounding structure were clear, the glomerulus contained a large number of capillaries, the renal tubules were full, and the balloon cavity was clearly visible. In contrast, the cisplatin group had severe renal injury, which

https://doi.org/10.1021/acsomega.2c04142
ACS Omega 2022, 7, 37401−37409

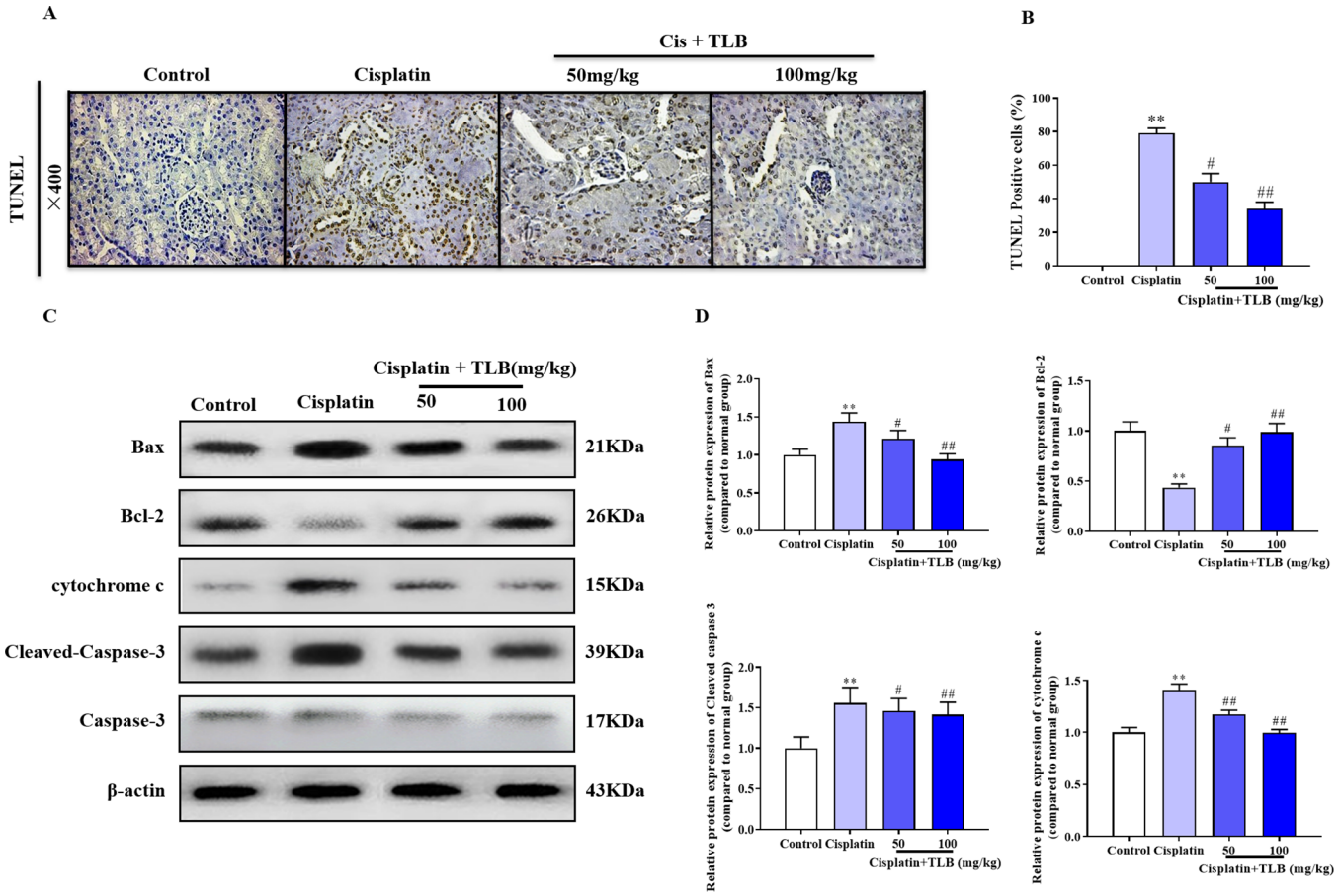

Figure 4. Pretreatment with TLB protected against apoptosis induced by cisplatin. Effects of TLB on apoptosis of renal cells in cisplatin-treated mice. Renal tissues stained with TUNEL staining (400×) (A). The presence of TUNEL-positive cells were evaluated using an image analyzer (B). The protein expressions of Bax, Bcl-2, cytochrome c, and caspase 3 (C) were detected by western blot in kidney tissues. The column chart shows antibody relative expression (D). The protein expression was examined by western blot analysis in kidney tissues from control, cisplatin, cisplatin + TLB (50 mg/kg), and cisplatin + TLB (100 mg/kg). All data were expressed as mean ± SD, $n = 8$. $^{**}p < 0.01$ vs control group; $^{\#}p < 0.05$, and $^{\#\#}p < 0.01$ vs cisplatin group.

mainly manifested as proximal renal tubular damage, detachment of renal tubular epithelial cells, glomerular congestion, renal tubular dilation, and a large amount of inflammatory infiltration. However, TLB pretreatment significantly improved these pathological changes, especially the high-dose TLB group (100 mg/kg) ($p < 0.01$) (Figure 2B). These results confirmed that TLB has an effective protective effect on cisplatin-induced kidney injury.

To further explore the effect of TLB on AKI induced by cisplatin, we determined the serum contents in CRE and BUN. Our data showed that after cisplatin injection, compared with the control group, both serum BUN (Figure 2C) and CRE (Figure 2D) levels were significantly increased ($p < 0.01$), which indicated that the cisplatin-induced mouse AKI model was successfully established. Compared with the cisplatin group, the levels of BUN and CRE in the TLB administration group were significantly decreased ($p < 0.05$, $p < 0.01$), which suggested that TLB has a significant protective effect on cisplatin-induced kidney damage in mice.

The previous studies indicated that, concomitant with renal dysfunction and histological damage, the serum contents of oxidative stress-related indicators also change significantly in mice.[23−25] In our study, compared with the control group, cisplatin exposure results in the decrease of SOD and CAT activity (Figure 2E,F) ($p < 0.01$) and the GSH content (Figure 2G) ($p < 0.05$) in the kidney tissues, while the content of MDA (Figure 2H) was increased significantly ($p < 0.01$). The results above further indicate that the mouse kidneys were obviously damaged. The indicators of the mice in the TLB administration groups tended toward the control group to varying degrees. The results above indicated that TLB exerts a protective effect on cisplatin-induced AKI in mice.

3.2. TLB Regulated the Expression of the MAPK Signaling Pathway in Cisplatin-Treated Mice. To further explore the protective mechanism of TLB pretreatment on cisplatin-induced AKI, we used western blot to investigate the effects of MAPK signaling pathways. As shown in Figure 3, injection with cisplatin increased the expression level of p-JNK, p-AKT, p-38, and p-ErK in kidney tissues compared with the control group ($p < 0.01$). However, the expression levels of these proteins were recovered after continuous administration of TLB for 10 days ($p < 0.05$, $p < 0.01$). The data indicated that TLB could alleviate cisplatin-induced kidney injury by improving the expression of the MAPK signaling pathway.

3.3. TLB Inhibits Cisplatin-Induced Apoptosis in Mice. To determine whether necrosis would coexist with apoptosis in cisplatin-induced nephrotoxicity, TUNEL staining was used to confirm and quantify the apoptosis in renal cells. As shown in Figure 4A, compared to the control group, the number of TUNEL-positive tubular cells was significantly increased in the

https://doi.org/10.1021/acsomega.2c04142
ACS Omega 2022, 7, 37401−37409

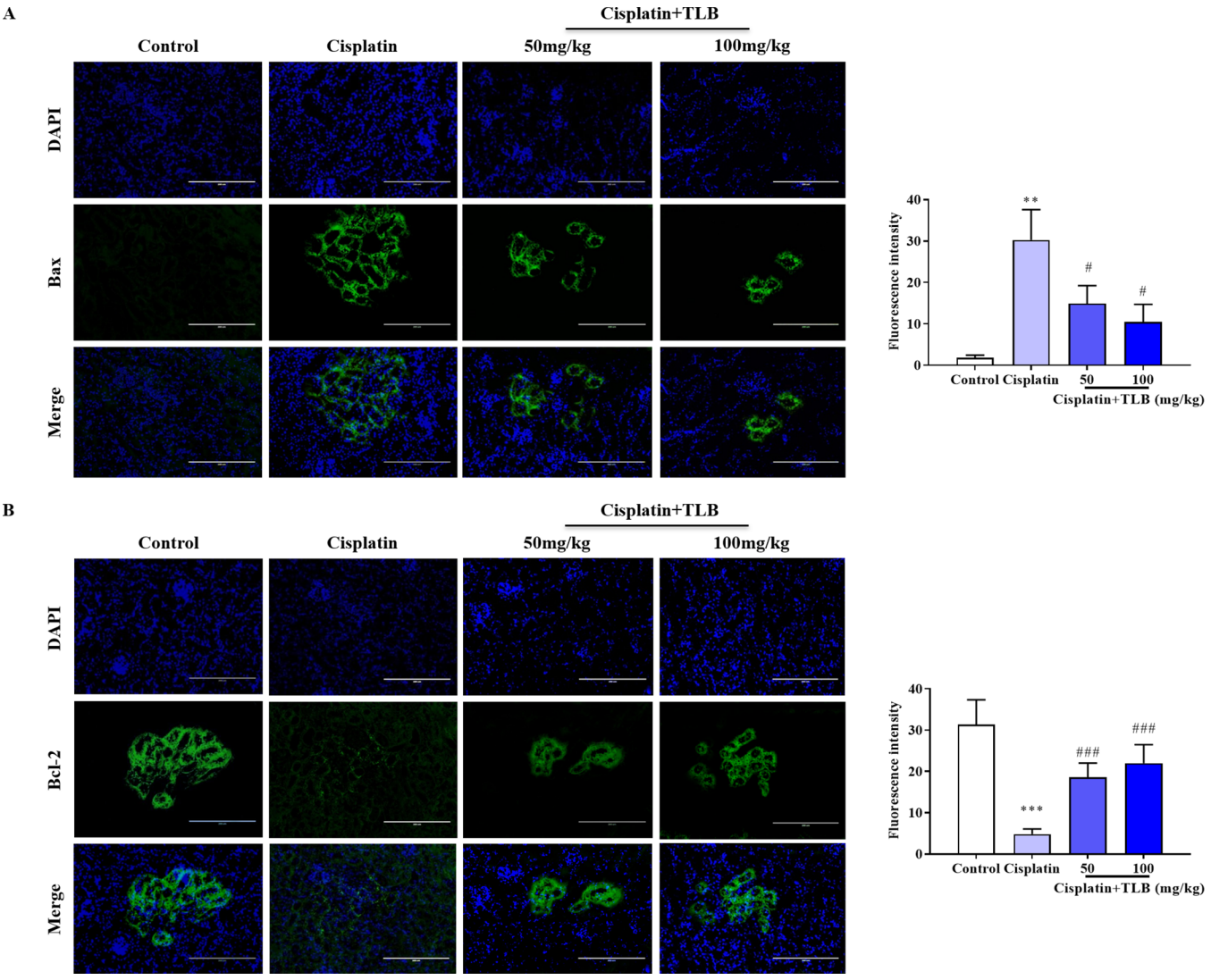

Figure 5. Effects of TLB on the expression of Bax (A)and Bcl-2 (B) in kidney tissues, and the fluorescence intensities were quantified. The expression level of Bax and Bcl-2 (green) in the tissue section isolated from different groups was evaluated with immunofluorescence. Representative immunofluorescence images were taken at 400 × DAPI (blue) acted as a nuclear counterstain. All data were expressed as mean ± SD, $n = 8$. $^{**}p < 0.01$, $^{***}p < 0.001$ vs control group; $^{\#}p < 0.05$, and $^{\#\#\#}p < 0.001$ vs cisplatin group.

model group. Pretreatment with TLB significantly decreased apoptotic cell numbers ($p < 0.05$, $p < 0.01$) (Figure 4B). The results proved that TLB may play a protective role by alleviating cisplatin-induced apoptosis of renal cells. To further verify the antiapoptotic mechanism of TLB in cisplatin-treated mice, western blot analysis was used to detect the expression of apoptosis-related proteins, such as cleaved-caspase-3, Bax, and Bcl-2. In Figure 4C, compared with the control group, the expressions of Bax, cleaved-caspase-3, and cytochrome c were significantly increased in the kidney tissue of the cisplatin-treated group ($p < 0.01$), and the expression of Bcl-2 was notably reduced ($p < 0.01$). After TLB treatment, the expression levels of these proteins were reversed to varying degrees ($p < 0.05$, $p < 0.01$), indicating that TLB can alleviate cisplatin-induced renal injury by improving the expression of these signaling pathways.

To further confirm the mechanism of cisplatin-induced apoptosis in renal tissues, IHC analysis was used to observe apoptotic renal tissue cells in the present study. As shown in Figure 5, compared with the control group, the expression of Bax (proapoptotic protein) in the cisplatin group was significantly increased ($p < 0.01$), while the expression of Bcl-2 (antiapoptotic protein) was significantly decreased ($p < 0.001$). In addition, the expression of Bcl-2 was significantly increased ($p < 0.001$), and the rate of positive expression of Bax was markedly reduced ($p < 0.05$) by TLB treatment compared to the cisplatin group. The results above show that TLB can significantly inhibit cisplatin-induced renal apoptosis by improving the expression of signaling pathways such as Bax and Bcl-2 etc.

4. DISCUSSION

The kidney is the major excretory organ of human body, when affected by external adverse factors; the kidney could be damaged to a different extent.[26] AKI is a common kidney disease caused by many factors, including nephrotoxic drug intake, sepsis, hypertension, and diabetes. Globally, more than 2 million people die because of AKI each year.[27,28] According to incomplete statistics, drugs with nephrotoxicity in hospitals account for more than 20%, and the incidence of drug-induced

https://doi.org/10.1021/acsomega.2c04142
ACS Omega 2022, 7, 37401−37409

kidney injury in the elderly is 66%.[16] Cisplatin, as a chemotherapy drug, is widely used in the clinical treatment of various solid tumors,[23] such as oophoroma, breast cancer, lung carcinoma, and HPV.[29] However, the nephrotoxicity caused by cisplatin greatly limits its clinical application. How to alleviate the nephrotoxicity of cisplatin to improve its chemotherapy effect has always been an important research topic. We constructed an in vivo AKI model and found that TLB could significantly improve cisplatin-induced AKI.

Increasing evidence suggests that the apoptosis of renal tubular cells is one of the main features of kidney injury caused by cisplatin, which causes necrosis of renal tubular cells and renal dysfunction.[30,31] In our study, H&E staining showed that cisplatin exposure caused necrosis of renal tubular cells, as well as inflammatory infiltration of lymphocytes around the central vein, and TLB can significantly reduce these renal tissue lesions. In addition, compared with the control group, CRE and BUN levels were significantly higher in the cisplatin group, indicating a decrease in glomerular filtration rate. Previous studies have shown that, concomitant with renal dysfunction and histological damage, cisplatin exposure increased MDA levels and reduced SOD, GSH, and CAT levels significantly.[32−34] Preadministration of TLB significantly improved these symptoms and pathological changes. The above results indicated the successful establishment of the cisplatin-induced kidney injury model in vivo and protective effect of TLB in cisplatin-mediated nephrotoxicity.

Previous studies have found that the activation of JNK (phospho-JNK) after cisplatin treatment aggravates renal function and causes cell apoptosis and tubular inflammation, suggesting the mechanism of JNK in nephrotoxicity.[35−37] One study showed that cisplatin injection can cause phosphorylation and accumulation of Erk MAPK in the mitochondria of proximal tubular epithelial cells.[36] A study has shown that blocking p38 MAPK activation alleviates cisplatin-mediated oxidative stress, inflammation, and apoptosis in the kidneys.[37] Therefore, the analysis of the MAPK pathway may be of great significance to explore new therapeutic measures to reduce cisplatin-induced kidney injury in mice. In our study, phosphorylation of JNK, p38, and Erk increased in the kidneys of mice modeled with cisplatin, indicating increased apoptosis. TLB administration for 1 week has reduced these levels, demonstrating that TLB reduced the formation of phosphorylation and reduced the activation of apoptotic pathways. The TLB administration can reverse this phenomenon and play a protective role.

To further explore the effect of TLB on renal apoptosis induced by cisplatin, TUNEL staining was used to confirm and quantify renal cell apoptosis. The results showed that compared with the control group, the number of TUNEL-positive tubule cells in the cisplatin group was significantly increased, indicating that cisplatin did induce renal cell apoptosis. At the same time, TLB pretreatment could significantly reduce the number of apoptotic cells. Mechanistically, cisplatin-induced nephrotoxicity involves two main apoptotic pathways: one is the endogenous pathway, and another is the regulation of downstream genes of the Bcl-2 family. The increased expressions of proapoptotic proteins of the Bcl-2 family and the decline of antiapoptotic proteins are the main manifestation.[38−41] When the expression levels of Bax are increased, Bax can form a homologous dimer with Bcl-2 and cleaved caspase3, finally promoting apoptosis. Therefore, as an apoptotic marker, caspase3 plays a key role in cisplatin-induced renal cell apoptosis. Therefore, improving cisplatin-induced renal cell apoptosis is an important target to alleviate cisplatin-induced nephrotoxicity.[42] Furthermore, numerous studies have shown that the activated AKT, as an upstream signal of apoptosis, could regulate its downstream target proteins such as Bcl-2 and Bax to inhibit apoptosis.[43] Cisplatin accumulates the ROS-dependent mitochondrial dysfunction in renal tubular cells and further promotes the release of apoptotic factors (such as Bax, Bcl-2, cytochrome c, and caspase family) and triggers apoptosis.[32] In our study, Western blotting analysis showed that the expression level of Bax, cytochrome c, and caspase-3 protein after cisplatin treatment was significantly higher than that of the control group, and TLB treatment significantly reduced these expression levels, suggesting that TLB can protect renal cells from cisplatin-induced apoptosis. In addition, further IHC analysis confirmed these results. The results above implied that TLB can significantly inhibit cisplatin-induced renal apoptosis by improving the expression of signaling pathways such as Bax, Bcl-2, and so on.

In addition, the indicators of the mice in the TLB administration group tended to different degrees to the control group, and the protection effect of the 100 mg/kg dose group was better, indicating that the TLB administration was dose-dependent. In conclusion, in the present work, TLB pretreatment markedly suppressed cisplatin-induced apoptosis. We have reason to think that administration of TLB may be considered as a therapeutic strategy to prevent cisplatin-induced acute renal injury.

AUTHOR INFORMATION

Corresponding Authors

Li-Chun Zhao − *College of Pharmacy, Guangxi University of Chinese Medicine, Nanning 530001, China*; Phone: +86-431-84533358; Email: hyzlc@126.com

Wei Li − *College of Chinese Medicinal Materials, Jilin Agricultural University, Changchun 130118, China; National and Local Joint Engineering Research Center for Ginseng Breeding and Development, Changchun 130118, China*; orcid.org/0000-0002-2988-4298; Phone: +86-431-84533304; Email: liwei7727@126.com

Authors

Yue-yang Duan − *College of Chinese Medicinal Materials, Jilin Agricultural University, Changchun 130118, China; National and Local Joint Engineering Research Center for Ginseng Breeding and Development, Changchun 130118, China*

Xiao-jie Mi − *College of Chinese Medicinal Materials, Jilin Agricultural University, Changchun 130118, China; Graduate School of Biotechnology, and College of Life Science, Kyung Hee University, Gyeonggi-do 17104, Republic of Korea*

Wen-ya Su − *College of Chinese Medicinal Materials, Jilin Agricultural University, Changchun 130118, China*

Shan Tang − *College of Chinese Medicinal Materials, Jilin Agricultural University, Changchun 130118, China*

Shuang Jiang − *College of Chinese Medicinal Materials, Jilin Agricultural University, Changchun 130118, China*

Zi Wang − *College of Chinese Medicinal Materials, Jilin Agricultural University, Changchun 130118, China*

Complete contact information is available at: https://pubs.acs.org/10.1021/acsomega.2c04142

https://doi.org/10.1021/acsomega.2c04142
ACS Omega 2022, 7, 37401−37409

Notes

The authors declare no competing financial interest.

■ ACKNOWLEDGMENTS

This work was supported by the grants of the National Natural Science Foundation of China (81860691); Guangxi Key Laboratory of Quality Standards for Traditional Chinese Medicines (Guizhong Reopening 201902); the Natural Science Foundation of Guangxi Province (2020GXNSFAA238021); and Key Projects of Guangxi Natural Science Foundation of (2021GXNSFDA075008).

■ ABBREVIATIONS

TLB	trilobatin
AKI	acute kidney injury
H&E	hematoxylin and eosin
BUN	blood urea nitrogen
Cr	creatinine
Bax	Bcl-2 associated X protein
Bcl-2	B-cell-lymphoma-2
MDA	malondialdehyde
GSH	glutathione
CAT	catalase
SOD	superoxide dismutase
ROS	reactive oxygen species
DAPI	6 diamidino-2-phenylindole
MAPK	mitogen-activated protein kinase
Akt	protein kinase B

■ REFERENCES

(1) Hou, S. Z.; Chen, S. X.; Huang, S.; Jiang, D. X.; Zhou, C. J.; Chen, C. Q.; Liang, Y. M.; Lai, X. P. The hypoglycemic activity of Lithocarpus polystachyus Rehd. leaves in the experimental hyperglycemic rats. *J. Ethnopharmacol.* **2011**, *138*, 142−149.

(2) Gao, J.; Liu, S.; Xu, F.; Liu, Y.; Lv, C.; Deng, Y.; Shi, J.; Gong, Q. Trilobatin Protects Against Oxidative Injury in Neuronal PC12 Cells Through Regulating Mitochondrial ROS Homeostasis Mediated by AMPK/Nrf2/Sirt3 Signaling Pathway. *Front. Mol. Neurosci.* **2018**, *11*, 267.

(3) Li, X.; Zhao, Y.; Huang, S.; Song, W.; Zeng, X.; Hou, S. Z.; Lai, X. P. New dihydrochalcone and propenamide from Lithocarpus polystachyus. *Nat. Prod. Commun.* **2014**, *9*, 653−654.

(4) Ning, R.; Wang, H.; Shen, Y.; Chen, Z.; Zhang, R.; Leng, Y.; Zhao, W. J. B.; Letters, M. C. Lithocarpic acids O-S, five homocycloartane derivatives from the cupules of Lithocarpus polystachyus. 2014, *24* (23), 5395−5398, DOI: 10.1016/j.bmcl.2014.10.036.

(5) Koh, G.; McCutcheon, K.; Zhang, F.; Liu, D.; Cartwright, C.; Martin, R.; Yang, P.; Liu, Z. Improvement of obesity phenotype by Chinese sweet leaf tea (Rubus suavissimus) components in high-fat diet-induced obese rats. *J. Agric. Food Chem.* **2011**, *59*, 98−104.

(6) Duge de Bernonville, T.; Guyot, S.; Paulin, J. P.; Gaucher, M.; Loufrani, L.; Henrion, D.; Derbre, S.; Guilet, D.; Richomme, P.; Dat, J. F.; Brisset, M. N. Dihydrochalcones: Implication in resistance to oxidative stress and bioactivities against advanced glycation end-products and vasoconstriction. *Phytochemistry* **2010**, *71*, 443−452.

(7) Hsu, C. Y. Yes, AKI truly leads to CKD. *J. Am. Soc. Nephrol.* **2012**, *23*, 967−969.

(8) Bucaloiu, I. D.; Kirchner, H. L.; Norfolk, E. R.; Hartle, J. E., 2nd; Perkins, R. M. Increased risk of death and de novo chronic kidney disease following reversible acute kidney injury. *Kidney Int.* **2012**, *81*, 477−485.

(9) Chen, C.-H.; Huang, Y.-C.; Lee, Y.-H.; Tan, Z.-L.; Tsai, C.-J.; Chuang, Y.-C.; Tu, H.-F.; Liu, T.-C.; Hsu, F.-T. Anticancer Efficacy and Mechanism of Amentoflavone for Sensitizing Oral Squamous Cell Carcinoma to Cisplatin. *Anticancer Res.* **2020**, *40*, 6723−6732.

(10) Lou, J.-S.; Zhao, L.-P.; Huang, Z.-H.; Chen, X.-Y.; Xu, J.-T.; Tai, W. C.-S.; Tsim, K. W. K.; Chen, Y.-T.; Xie, T. Ginkgetin derived from Ginkgo biloba leaves enhances the therapeutic effect of cisplatin via ferroptosis-mediated disruption of the Nrf2/HO-1 axis in EGFR wild-type non-small-cell lung cancer. *Phytomedicine* **2021**, *80*, No. 153370.

(11) Kelland, L. The resurgence of platinum-based cancer chemotherapy. *Nat. Rev. Cancer* **2007**, *7*, 573−584.

(12) Delord, J.-P.; Puozzo, C.; Lefresne, F.; Bugat, R. Combination chemotherapy of vinorelbine and cisplatin: a phase I pharmacokinetic study in patients with metastatic solid tumors. *Anticancer Res.* **2009**, *29*, 553−560.

(13) Miller, R. P.; Tadagavadi, R. K.; Ramesh, G.; Reeves, W. B. Mechanisms of Cisplatin nephrotoxicity. *Toxins* **2010**, *2*, 2490−2518.

(14) Kong, M. J.; Bak, S. H.; Han, K. H.; Kim, J. I.; Park, J. W.; Park, K. M. Fragmentation of kidney epithelial cell primary cilia occurs by cisplatin and these cilia fragments are excreted into the urine. *Redox Biol.* **2018**, *20*, 38−45.

(15) Saifi, M. A.; Sangomla, S.; Khurana, A.; Godugu, C. Protective Effect of Nanoceria on Cisplatin-Induced Nephrotoxicity by Amelioration of Oxidative Stress and Pro-inflammatory Mechanisms. *Biol. Trace Elem. Res.* **2019**, *189*, 145−156.

(16) Pabla, N.; Dong, Z. Cisplatin nephrotoxicity: mechanisms and renoprotective strategies. *Kidney Int.* **2008**, *73*, 994−1007.

(17) Liu, Z.; Li, H.; Su, J.; Xu, S.; Zhu, F.; Ai, J.; Hu, Z.; Zhou, M.; Tian, J.; Su, Z.; Yang, P.; Nie, J. Numb Depletion Promotes Drp1-Mediated Mitochondrial Fission and Exacerbates Mitochondrial Fragmentation and Dysfunction in Acute Kidney Injury. *Antioxid. Redox Signaling* **2018**, *30*, 1797−1816.

(18) Gomes, A.; Couto, D.; Alves, A.; Dias, I.; Freitas, M.; Porto, G.; Duarte, J. A.; Fernandes, E. Trihydroxyflavones with antioxidant and anti-inflammatory efficacy. *Biofactors* **2012**, *38*, 378−386.

(19) Malik, S.; Suchal, K.; Gamad, N.; Dinda, A. K.; Arya, D. S.; Bhatia, J. Telmisartan ameliorates cisplatin-induced nephrotoxicity by inhibiting MAPK mediated inflammation and apoptosis. *Eur. J. Pharmacol.* **2015**, *748*, 54−60.

(20) Hu, J.-N.; Yang, J.-Y.; Jiang, S.; Zhang, J.; Liu, Z.; Hou, J.-G.; Gong, X.-J.; Wang, Y.-P.; Wang, Z.; Li, W. Panax quinquefolium saponins protect against cisplatin evoked intestinal injury via ROS-mediated multiple mechanisms. *Phytomedicine* **2021**, *82*, No. 153446.

(21) Yang, J.; Zhong, Y.; Hao, W.; Liu, X.; Shen, Q.; Li, Y.; Ren, S.; Wang, Z.; Li, W.; Zhao, L. C. The PI3K/Akt and NF-κB signaling pathways are involved in the protective effects of Lithocarpus polystachyus (sweet tea) on APAP-induced oxidative stress injury in mice. *RSC Adv.* **2020**, *10*, 18044−18053.

(22) Domitrović, R.; Cvijanović, O.; Pernjak-Pugel, E.; Skoda, M.; Mikelić, L.; Crnčević-Orlić, Z. Berberine exerts nephroprotective effect against cisplatin-induced kidney damage through inhibition of oxidative/nitrosative stress, inflammation, autophagy and apoptosis. *Food Chem. Toxicol.* **2013**, *62*, 397−406.

(23) Chtourou, Y.; Aouey, B.; Aroui, S.; Kebieche, M.; Fetoui, H. Anti-apoptotic and anti-inflammatory effects of naringin on cisplatin-induced renal injury in the rat. *Chem. Biol. Interact.* **2016**, *243*, 1−9.

(24) Huang, J.; Bao, D.; Lei, C.; Tang, H.; Zhang, C.; Su, H.; Zhang, C. J. F. Selenoprotein T protects against cisplatin-induced acute kidney injury through suppression of oxidative stress and apoptosis. *FASEB J.* **2020**, *34*, 11983−11996.

(25) Gu, H.; Gwon, M.-G.; Kim, J.; Leem, J.; Lee, S. J. Oridonin Attenuates Cisplatin-Induced Acute Kidney Injury via Inhibiting Oxidative Stress, Apoptosis, and Inflammation in Mice. *Biomed. Res. Int.* **2022**, *2022*, No. 3002962.

(26) Karakoc, H. T. E.; Altintas, R.; Parlakpinar, H.; Polat, A.; Samdanci, E.; Sagir, M.; Duran, Z. R. Protective Effects of Molsidomine Against Cisplatin-Induced Nephrotoxicity. *Adv. Clin. Exp. Med.* **2015**, *24*, 585−593.

(27) Ueki, M.; Ueno, M.; Morishita, J.; Maekawa, N. Curcumin ameliorates cisplatin-induced nephrotoxicity by inhibiting renal inflammation in mice. *J. Biosci. Bioeng.* **2013**, *115*, 547−551.

https://doi.org/10.1021/acsomega.2c04142
ACS Omega 2022, 7, 37401−37409

(28) Peres, L. A. B.; da Cunha, A. D., Jr. Acute nephrotoxicity of cisplatin: molecular mechanisms. *J. Bras. Nefrol.* **2013**, *35*, 332−340.
(29) Oberoi, H. S.; Nukolova, N. V.; Laquer, F. C.; Poluektova, L. Y.; Huang, J. G.; Alnouti, Y.; Yokohira, M.; Arnold, L. L.; Kabanov, A. V.; Cohen, S. M.; Bronich, T. K. Cisplatin-loaded core cross-linked micelles: comparative pharmacokinetics, antitumor activity, and toxicity in mice. *Int. J. Nanomed.* **2012**, *7*, 2557−2571.
(30) Chen, X.; Wei, W.; Li, Y.; Huang, J.; Ci, X. Hesperetin relieves cisplatin-induced acute kidney injury by mitigating oxidative stress, inflammation and apoptosis. *Chem Biol Interact.* **2019**, *308*, 269−278.
(31) Aladaileh, S. H.; Al-Swailmi, F. K.; Abukhalil, M. H.; Ahmeda, A. F.; Mahmoud, A. M. Punicalagin prevents cisplatin-induced nephrotoxicity by attenuating oxidative stress, inflammatory response, and apoptosis in rats. 2021, *286*, 120071, DOI: 10.1016/j.lfs.2021.120071.
(32) Fernandez-Rojas, B.; Medina-Campos, O. N.; Hernandez-Pando, R.; Negrette-Guzman, M.; Huerta-Yepez, S.; Pedraza-Chaverri, J. C-Phycocyanin prevents cisplatin-induced nephrotoxicity through inhibition of oxidative stress. *Food Funct.* **2014**, *5*, 480−490.
(33) Kim, J. I.; Kim, J.; Jang, H. S.; Noh, M. R.; Lipschutz, J. H.; Park, K. M. Reduction of oxidative stress during recovery accelerates normalization of primary cilia length that is altered after ischemic injury in murine kidneys. 2013, *304* (10), F1283−F1294, DOI: 10.1152/ajprenal.00427.2012.
(34) Han, S. J.; Jang, H.-S.; Seu, S. Y.; Cho, H.-J.; Hwang, Y.-J.; Kim, J. I.; Park, K. M. Hepatic ischemia/reperfusion injury disrupts the homeostasis of kidney primary cilia via oxidative stress. 2017, *1863* (7), 1817−1828, DOI: 10.1016/j.bbadis.2017.05.004.
(35) Rabb, H.; Griffin, M. D.; McKay, D. B.; Swaminathan, S.; Pickkers, P.; Rosner, M. H.; Kellum, J. A.; Ronco, C.; Acute Dialysis Quality Initiative Consensus XIII Work Group. Inflammation in AKI: Current Understanding, Key Questions, and Knowledge Gaps. *J. Am. Soc. Nephrol.* **2016**, *27*, 371−379.
(36) Kim, H. Y.; Okubo, T.; Juneja, L. R.; Yokozawa, T. The protective role of amla (Emblica officinalis Gaertn.) against fructose-induced metabolic syndrome in a rat model. *Br. J. Nutr.* **2010**, *103*, 502−512.
(37) Ma, X.; Dang, C.; Kang, H.; Dai, Z.; Lin, S.; Guan, H.; Liu, X.; Wang, X.; Hui, W. Saikosaponin-D reduces cisplatin-induced nephrotoxicity by repressing ROS-mediated activation of MAPK and NF-κB signalling pathways. 2015, *28* (1), 399−408, DOI: 10.1016/j.intimp.2015.06.020.
(38) Forgione, M. A.; Cap, A.; Liao, R.; Moldovan, N. I.; Eberhardt, R. T.; Lim, C. C.; Jones, J.; Goldschmidt-Clermont, P. J.; Loscalzo, J. Heterozygous cellular glutathione peroxidase deficiency in the mouse: abnormalities in vascular and cardiac function and structure. *Circulation* **2002**, *106*, 1154−1158.
(39) Satoh, M.; Kashihara, N.; Fujimoto, S.; Horike, H.; Tokura, T.; Namikoshi, T.; Sasaki, T.; Makino, H. A novel free radical scavenger, edarabone, protects against cisplatin-induced acute renal damage in vitro and in vivo. *J. Pharmacol. Exp. Ther.* **2003**, *305*, 1183−1190.
(40) Wei, Q.; Dong, G.; Franklin, J.; Dong, Z. The pathological role of Bax in cisplatin nephrotoxicity. *Kidney Int.* **2007**, *72*, 53−62.
(41) El-Awady, E.-S.; Moustafa, Y.; Abo-Elmatty, D.; Radwan, A. Cisplatin-induced cardiotoxicity: Mechanisms and cardioprotective strategies. 2011, *650* (1), 335−341, DOI: 10.1016/j.ejphar.2010.09.085.
(42) Ali, B. H.; Al-Salam, S.; Al Za'abi, M.; Al Balushi, K. A.; AlMahruqi, A. S.; Beegam, S.; Al-Lawatia, I.; Waly, M. I.; Nemmar, A. Renoprotective effects of gamma-aminobutyric acid on cisplatin-induced acute renal injury in rats. *Basic Clin. Pharmacol. Toxicol.* **2015**, *116*, 62−68.
(43) Saad, A. A.; Youssef, M. I.; El-Shennawy, L. K. Cisplatin induced damage in kidney genomic DNA and nephrotoxicity in male rats: the protective effect of grape seed proanthocyanidin extract. *Food Chem. Toxicol.* **2009**, *47*, 1499−1506.

https://doi.org/10.1021/acsomega.2c04142
ACS Omega 2022, 7, 37401−37409